Civil Engineering Infrastructures Journal xx,xx

DOI: 10.22059/ceij.2025.377637.2075

Influence of Anchor Aspect Ratio on Geocell Reinforced Anchor Capacity Using 3D Finite Element Analysis

by

Ashutosh Kumar
Research Scholar
Department of Civil Engineering
National Institute of Technology Jamshedpur
Jamshedpur - 831014, India
e-mail: kumar.90civil@gmail.com

Mukesh Kumar
M.Tech
Department of Civil Engineering
National Institute of Technology Jamshedpur
Jamshedpur - 831014, India
e-mail: mukeshjayshwal1997@gmail.com

Dr. Awdhesh Kumar Choudhary (***Corresponding Author**)
Assistant Professor
Department of Civil Engineering
National Institute of Technology Jamshedpur
Jamshedpur - 831014, India
e-mail: awdhesh.ce@nitjsr.ac.in

and

Prof. Anil Kumar Choudhary
Professor
Department of Civil Engineering
National Institute of Technology Jamshedpur
Jamshedpur - 831014, India
e-mail: akchoudhary.ce@nitjsr.ac.in

***Corresponding Author**

Contact Address: Dr. Awdhesh Kumar Choudhary
Assistant Professor
Department of Civil Engineering
National Institute of Technology Jamshedpur
Jamshedpur - 831014, India
e-mail: awdhesh.ce@nitjsr.ac.in

Manuscript Submitted to the ***Civil Engineering Infrastructures Journal***.

Received: 14/06/2024

Revised: 12/04/2025

Accepted: 30/04/2025

Abstract

Vertical anchor plates are commonly employed to counteract lateral pullout forces in structures like sheet pile walls, retaining walls, bulkheads, and abutments for railways and highways etc thereby imparting stability to these structures by restricting the lateral movement. In the present study, the influence of the vertical anchor plate's aspect ratio, placed in unreinforced and geocell reinforced soil mass have been studied through a series of 3D numerical analysis. It has been observed that the load-carrying capacity of anchor plate is greatly influenced by the aspect ratio of anchor plate. The pullout factor was found to decrease with an increase in L/h up to 5, beyond which decrement was found to be marginal. This indicates that the load-carrying behaviour of the vertical anchor plate shifted from square to strip. Further, the performance of vertical anchor plates significantly increases in the range of 146%-227% with the use of geocell reinforcement for different aspect ratios of an anchor plate. However, the maximum performance improvement was found to be nearly 227% for an aspect ratio (i.e., L/h) of 3, demonstrating that the rectangular anchor plate having an aspect ratio of 3 placed in geocell reinforced soil mass performed better among others.

Keywords: Vertical anchor plate; Aspect ratio; Pullout factor; Geocell; FEM

Introduction

The numerous geotechnical engineering concepts gain popularity and significant attention to onshore and offshore structures. The geotechnical structures such as, sheet pile wall, retaining wall, bulkhead, bridge abutments, diaphragm walls etc. are example of onshore construction activities. These type of structures generally experience a large lateral force. So to restrict the lateral forces, vertical anchor plates are predominantly used. The vertical anchor plate consists of an iron plate which is connected to the retaining structures through the tie rod that effectively distributes the pullout force to the soil around. The pullout capacity of anchors depends on multiple factors, including soil characteristics, density, embedment depth, and the anchor plate's dimensions and geometry. A comprehensive review of anchor plates and their uses in geotechnical engineering structures is provided by Das and Shukla (2013). Multiple studies were conducted to evaluate the effect of different parameters on the performance of vertical anchor plates in unreinforced soil systems (kumar and Sahoo 2012; Choudhary et al., 2019; Zhuang et al., 2021; Zhang et al., 2022; Tilak and Samadhiya 2022). Shahriar et al. (2020) developed an analytical approach to determine the maximum pullout capacity of vertical anchors in cohesionless soils, accounting for 3D failure mechanisms, anchor surface roughness, and material properties. Xing et al. (2023) determined the limiting values of shape factors for vertically loaded anchors at deep-embedded depths using the finite-element method. Results indicate that reducing the aspect ratio of a fluke decreases the limiting shape factor when the fluke area remains constant, while fluke area has minimal impact if the fluke length is constant.

Many times, it has been seen that when this anchor plate installed in weak soil or heavily loaded, the anchor often experiences shear failure resulting in the collapse of supported structure (LaGatta and Shield, 1984). Therefore, to enhance the pullout capacity and to avoid sudden failure it is utmost important to improve the soil in which these anchors embedded. There are various ground improvement techniques, amongst which soil reinforcement is the most popular sustainable technique being widely used to enhance the performance of soil mass.

Geocell reinforcement, which is newly developed in this field, facilitate sustainable solutions for the infrastructure development, particularly in improving the load carrying capacity of a geotechnical structure. Geocells are 3D structure polymeric interconnected cells filled with soil which provide excellent support to loads through all-around confinement and are widely used in a variety of geotechnical applications, including retaining walls, sheet pile walls, embankments, foundations, pavements, slopes, railways, and diaphragm walls (Dash, 2010; Mehdipour et al., 2013; Hegde and Sitharam, 2015a, 2015b; Indraratna et al., 2015; Oliaei and Kouzegaran, 2017; Song et al., 2022; Kumar et al., 2024). Employing geocell reinforcement in structures offers multiple advantages, including enhanced stability, improved resilience to environmental conditions, greater resistance to dynamic loads, erosion mitigation, foundation support, and reductions in project time and costs. Because of its versatile configuration, geocell is regarded as the most sustainable, adaptable, and environmentally friendly solution for several civil engineering structures (Krishna and Latha Madhavi G, 2023). In regards to the above, the possible application of geocell reinforcement as a sustainable material in improving the performance of vertical anchor plate system has been reported by Dash and Choudhary (2018, 2019). The above study is limited to the square anchor plate system. However, the performance of an anchor plate in unreinforced soil mass is greatly influence by the aspect ratio of the plate as reported in the past (Choudhary et al., 2019; Shahriar et al. 2020). Whereas, the load carrying capacity of vertical anchor plate having different aspect ratio embedded in geocell reinforced soil mass has not been reported systematically. Considering this, the impact of the vertical anchor plate's aspect ratio embedded in geocell-reinforced soil has been examined using a series of three-dimensional numerical simulations. The specifics of these analyses are elaborated in the subsequent section.

Numerical model

In order to evaluate the behavior of anchor plates, a finite element model was developed with the aid of PLAXIS 3D software to investigate the impact of the aspect ratio of vertical anchor plates in both unreinforced and reinforced sand. The PLAXIS 3D is a three-dimensional finite element programme that includes an integrated PLAXIS library with numerous constitutive and structural models as well as the capacity to perform sensitive analysis on a broad range of geotechnical engineering problems. Since it produces a second-order interpolation of displacements, a tetrahedral element with ten nodes was adopted in this study to developed a 3-D finite element mesh.

All simulations were performed with an embedment ratio of 3 to replicate shallow anchor conditions. Spacious domains were utilized to minimize boundary effects. A finite element model tank, measuring 1.4 m in length, 1.6 m in width, and 0.5 m in height, was constructed. The anchor's length ranged from 1 to 6 times the anchor plate's height, set at 0.1 m. The plate thickness was fixed at 0.01 m. The anchor plate, crafted from rigid mild steel, was connected to a tie rod with a diameter of 0.012 m at its center. These model dimensions were adapted from the experimental setup reported by Dash and Choudhary (2018).

The finite element mesh was generated with 10-node tetrahedral elements. To model soil behavior, a non-associative elasto-plastic approach, referred to as the Mohr-Coulomb (MC) constitutive model, was employed (PLAXIS 2019). Although more advanced constitutive models exist, the Mohr-Coulomb (MC) model was selected as suitable since its strength and yield characteristics rely on volumetric strain and stress levels, which are relevant to the measured pullout capacity. Besides, it has been shown that the MC constitutive laws are efficient and effective for simulating granular materials in a numerous geosynthetic applications (M. Rahimi et al., 2018; Ari and Misir, 2021). The following parameters are required to develop Mohr-Coulomb model in PLAXIS 3D: Young's modulus (E), friction angle

(ϕ), Poisson's ratio (ν), cohesion (c), and the dilatancy angle (ψ) which is a non-associate flow rule parameter.

A plate structural element from the PLAXIS 3D library, whose movement was constrained in the lateral direction to approximate a rough anchor plate, was used to model the anchor plate (Fig. 1). The anchor plate is assumed to be rigid because the stiffness of the anchor plate is quite higher than that of the soil. An embedded beam structural element from the PLAXIS 3D library was used to model the embedded beam. The square shape of the geocell having a pocket size of 100 mm was constructed. In PLAXIS 3D, the available geogrid element was used to build the soil reinforcement. Three degrees of freedom (u_x, u_y, u_z) for translation and six nodes characterise the triangular surface elements that comprise the geogrid mesh layout. The connecting nodes share the translational degrees of freedom when two geogrid elements are joined to one another. Geogrids are thin structural elements which are resistant to membrane stress but not bending stresses. It cannot withstand compression. However, it can only sustain tensile stresses. Since a geogrid element deforms in one dimension along its axial direction, the model's parameter distribution inside the material is consider to be isotropic. Hence, its constitutive relationship is therefore comparable to that of linear elastic. A similar method has previously been employed by a number of researchers to model geogrid reinforcement. (Hegde and Sitharam 2015a; Choudhary et al., 2019).

In PLAXIS 3D, the interface element is a critical tool for simulating the interaction between soil and structural elements, such as anchor plate, embedded beams, piles, or slabs. These zero-thickness elements are placed at contact surfaces to accurately capture relative movements, slippage, friction, or separation. The interface behavior is governed by properties like cohesion, friction angle, tensile strength, and stiffness parameters (normal and shear). A key parameter, the strength reduction factor (R_{inter}), scales the interface strength relative to the adjacent soil,

allowing for partial or perfect interaction modeling. Interface elements are widely used in geotechnical applications, including retaining structures, pile foundations, and tunnel linings, to ensure realistic stress transfer and deformation patterns at soil-structure boundaries. Therefore, for present study an interface element with virtual thickness of an imaginary dimension from the PLAXIS 3D library was used to assign the material properties of the interface in order to model the soil-structure interface interaction. The 12-node interface elements used to build the interfaces were compatible with the 6-noded soil components and were created after the mesh was generated. To establish the contact between the soil and the geocell during construction and use, interface components are placed between the two. The interface can be described as an elasto-plastic mode in order to represent the interaction. The interface's strength governs how stress is transferred. It is determined by multiplying the surrounding soil's strength by the friction coefficient Rinter between the soil and the interface element. As a result, the parameter R_{inter} has been used to indicate the interaction degree. Therefore, taking $R_{inter} = 0.7$, which is the ratio between the shear strength of the soil structural interface and the soil itself, has been used for the numerical analyses.

This numerical model was shown to be adequate for simulating the horizontal pullout behavior of anchor plates, with 19310 elements of 10 nodes totaling 30500 nodes for the unreinforced case and 22894 elements and 42560 nodes for the geocell reinforced case. It was discovered that a medium mesh with a 0.125 coarseness ratio encircled by a finer mesh was adequate. In order to observe the resistance that resulted from applying a series of preset displacements to the plate, the study was conducted using a displacement control type. It should be mentioned that because the anchor plate is fixedly attached to the tie rod, the tie rod and the plate anchor work as one unit. This means that the resistance created is constant throughout the composite system (i.e., plate anchor and tie rod). The load-displacement curve is used to calculate the capacity, which is then taken to be equal to the highest load at which the curve plateaus. The

pullout capacity of an anchor plate at a specific embedment depth is defined as the load at which the load-displacement graph achieves a plateau or the displacement reaching about 7.5% of the plate height, whichever comes first. The cross-sectional view of anchor plate, the plan of anchor plate, and the generated mesh and the model domains with boundary conditions with interface elements surrounding the anchor plate with geocell reinforcement are depicted in Fig. 1. The material properties for the soil, anchor plate with tie rod, and geocell in this study were adopted from Dash and Choudhary (2018) and are detailed in Tables 1, 2, and 3, respectively.

Results and Discussions

Finite element model validation

Assessing the quality and precision of the current model created in PLAXIS 3D is crucial prior to presenting an in-depth numerical analysis. Dash and Choudhary (2018) experimental data has been verified. The brief description of the experimental study as reported by Dash and Choudhary (2018) are discussed here for better understanding. A vertical square anchor plate having a dimension of 100 mm (Length) x 100 mm (Width) and 10 mm (Thickness) was adopted for the study. A tie rod of 12 mm in diameter was connected at the center of the anchor plate. The placing of the sand was done using the pluviation technique. The test was conducted in a laminar box whose internal dimension is 1400 mm long, 1600 mm wide and 1100 mm deep. The anchor plate was placed at 200 mm from rear side and 200 mm from bottom of the tank. The geocell of nearly square shape having pocket size 100 mm and height 200 mm as placed in front of the anchor plate. The number of geogrid cells is 21. The experimental setup used is shown in Fig. 2. The analysis has been carried by developing numerical model keeping all the properties of soil and reinforcement similar to the experimental study. The derived results are compared with physical model test data, as shown in Fig. 3, for both unreinforced

and geocell-reinforced cases, expressed as the non-dimensional pullout factor (N_u). The term pullout factor can be defined as

$$Nu = \frac{Q}{\Upsilon AH} \quad (1)$$

where, N_u is pullout factor, Q is the pullout load, where the soil's unit weight is denoted by ϒ, the anchor plate's plan area by A, and the embedment depth by H. As illustrated in Fig. 3, the numerical outcomes for both unreinforced and geocell-reinforced scenarios exhibit strong agreement with experimental findings from Dash and Choudhary (2018). For example, for unreinforced case, at 10 % displacement, the numerical and experimental value found to be nearly same i.e., 27 and 28, respectively whereas for reinforced case these values found to be nearly 56 (numerical) and 53 (experiment), the differences in the order of 5.6%. The differences so obtained for the unreinforced case are marginal. However, for the reinforced case, the numerical value so obtained shows little deviations from the experimental value at higher anchor displacement. This could be the consequence of mistakes made when identifying the properties of the soil, especially the soil modulus, which affects the initial settlement. However, the obtained peak friction angle might be accurate, yielding nearly same pullout factor (N_u) for both the cases. Additionally, the numerical analysis curve for geocell-reinforced soil showed minor deviations from physical model test data, possibly attributed to the composite stiffness of the soil and geocell system. Therefore, it can be said that the suggested 3D model is capable of precisely predicting how an anchor will behave in both reinforced and unreinforced anchor systems. The performance of the geocell-reinforced anchor system and the impact of critical parameters on its overall behavior, discussed in the subsequent section, can be analyzed using the present numerical model.

Influence of aspect ratio of anchor plate in unreinforced soil

Fig. 4 illustrates the characteristic pullout load-displacement behaviour of anchor plates embedded at a shallow depth (H/h = 3) with aspect ratios ranging from L/h = 1 to 6, where L is the anchor plate's length, *h* is the height of anchor plate and *H* is the embedment depth. To study the influence of change in length of anchor plate *(L)*, the anchor height, (*h)* was kept constant i.e., 100 mm. Fig. 4 makes it abundantly evident that the larger the anchor plate's area, the more soil mass is used to share the anchor load, increasing the system's total capacity. Furthermore, it is evident that in every instance, the anchor plate clearly fails at almost the same percentage of anchor displacement. Moreover, Fig. 5 displays the pullout factor, Nu, which is the non-dimensional expression of the pullout load, Q, as calculated from Fig. 4. As can be seen, each curve displays two distinct stages: Pullout factor advances steadily with anchor displacement during the first stage until it reaches the maximum resistance. Second, as the anchor plate moves horizontally further, the curve stays constant after reaching its apex. At L/h = 5, the pullout factor also rapidly drops as the vertical anchor plate's aspect ratio increases. Beyond L/h =5, further reduction in pullout factor found to be negligible. For example, the pullout factor decreases from 27.84 to 9.60 with increase in L/h ratio from 1 to 5 as presented in Table 4. However, further decrement found to be marginal (i.e., 9.11) with increase in L/h ratio to 6 (Table 4). The above observation clearly indicates that the anchor behaviour shifted from square to strip anchor case. The failure mechanism becomes nearly two-dimensional, resembling a plane strain condition. The failure surface extends primarily along the width of the strip anchor, reducing the influence of soil on the anchor's sides. There have also been prior reports of similar behaviour (Ghaly 1997; Rokonuzzaman and Sakai, 2012a, 2012b).

Influence of aspect ratio of anchor plate in geocell reinforced soil

Fig. 6 illustrates the effect of anchor plate aspect ratio (L/h = 1 to 7) in geocell-reinforced soil at a shallow embedment depth (H/h = 3). The results demonstrate a substantial increase in

pullout capacity with geocell reinforcement across all aspect ratios. However, increase in the anchor capacity found to be marginal beyond aspect ratio (i.e., L/h) of 5. This indicates that beyond aspect ratio of L/h = 5, the geocell reinforced anchor system seizes its strength to maximum value and no further yielding of strength mobilized. Similar trend can be observed through the Pullout factor versus pullout response as well (Fig. 7). The pullout factor diminishes as the anchor plate's aspect ratio increases. This is in general agreement observed for unreinforced case as well. Besides, the load-bearing capacity is mainly influenced by the width of the anchor, as the contribution from the side flanks diminishes with increasing length. The failure surface transitions to a more two-dimensional plane strain condition, reducing the contribution from the surrounding soil volume. The geocell reinforcement primarily interacts with the bottom surface of the anchor, leading to a pronounced improvement in bearing capacity compared to unreinforced case. Thus, it can be inferred that the behavior of a square anchor transitions to that of a strip anchor when the aspect ratio (L/h) exceeds 5 for a reinforced geocell anchor plate. This suggests that the effect of the anchor plate's aspect ratio is comparable in both unreinforced and reinforced scenarios. Comparable findings have been noted by various researchers (Ilamparuthi et al., 2008; Rahimi et al., 2018).

The summary of the numerical results for reinforced case has been presented in Table 5. It is evident that as the aspect ratio rises from L/h = 1 to 7, the peak pullout load increases from 3.89 kN to 7.86 kN whereas the pullout factor decreases significantly. The pullout factor decreases significantly, from 77.31 to 29.00, as the aspect ratio rises from L/h = 1 to L/h = 5, after which the rate of reduction slows with further increases in the anchor's aspect ratio. Furthermore, it is evident that, regardless of the anchor's aspect ratio, incorporating geocell reinforcement significantly boosts the anchor system's performance by 146% to 227%. The greatest enhancement, approximately 227%, occurs at an aspect ratio (L/h) of 3, indicating that a rectangular anchor plate with an L/h of 3 in geocell-reinforced soil outperforms other

configurations. The curve, shown in the Fig. 8 depicts the relationship between pullout factor (Nu) and aspect ratio. It is noted that the pullout factor steadily declines as the aspect ratio increases in both unreinforced and reinforced soil masses. However, the rate of reduction in pullout factor decreases beyond certain aspect ratio (i.e., L/h). This once again confirmed that the anchor behavior is very dependent on their aspect ratios which lead to decrease in the performance of system. The peak resistance in reinforced cases is notably higher than in unreinforced cases, indicating that geocell reinforcement, with its three-dimensional polymeric interconnected cells filled with soil, offers comprehensive confinement to the soil mass, thereby providing robust support to the anchor plate system. Additionally, it is evident that geocell reinforcement significantly enhances anchor capacity compared to unreinforced conditions, even for anchor plates with larger aspect ratios, as illustrated in Fig. 8.

Influence of aspect ratio of anchor plate on stress and displacement contour

To gain a deeper comprehension of the impact of aspect ratio and geocell reinforcement on the pullout response of vertical anchor plate, the displacement contours and the tensile strength contours' in geocell reinforcement can be analysed. Fig. 9 and 10, shows the lateral displacement contours for both the unreinforced and reinforced cases having anchor aspect ratio (L/h) of 1 (i.e., 100 mm × 100 mm) and 4 (i.e., 100 mm × 400 mm), respectively. It can be notice that the pattern of displacement contour for all the cases found to be nearly same that it generated from the bottom edge of the anchor plate, extended laterally and finally reached to the ground surface. Moreover, the anchor having aspect ratio (L/h) of 4, the displacement contours are elongated along the anchor's length and primarily confined to the width. The influence zone is shallower and narrower, as the load transfer is predominantly two-dimensional. However, it is interest to note that the flow of soil element confined within the geocell mattress for anchor aspect ratio L/h = 1 (Fig. 9b) and extended beyond the geocell

reinforcement for L/h = 4 (Fig. 10b) suggesting that a larger anchor plate distributes the applied load across a broader area, resulting in an expanded failure surface, which enhances resistance near geocell-reinforced anchor beds, thereby improving the system's overall performance. However, the maximum displacement for aspect ratio (L/h) of 1 and 4 for unreinforced case was found to be nearly 60 mm (Fig. 9a) and 72 mm (Fig. 10b), respectively. Whereas for reinforced case it has been reduces to 42 mm and 45 mm for the same aspect ratio. This is mainly due to the combine effect of geocell and the infill soil material forming a quasi-rigid layer to resists the upward soil movement and restricts the heave formation. Thus, it can be concluded that employing geocell reinforcement effectively confines the infill soil mass, limiting the outward movement of soil particles and thereby enhancing resistance, which ultimately increases the overall capacity of the reinforced anchor system.

Influence of aspect ratio of anchor on force and displacement contour of reinforcement

The tensile force distribution in geocell walls during horizontal pullout loading is illustrated in Fig. 10. The contours of tensile forces reveal that these forces are primarily concentrated at the front face of the geocell walls and are highly localized around the anchor plate when L/h = 1 (Fig. 10a). It is also noted that the tensile force distribution remains confined within the central pocket of the geocell mattress, without extending laterally. This could be mainly because of high stress concentration created by the anchor plate at the centre leading to higher tensile forces in the reinforcement. Whereas, almost entire geocell mattress experiences tensile forces for aspect ratio of 4, suggesting that with increase in the aspect ratio, the large portion of composite structures (i.e., geocell reinforced system) involve in sharing anchor load leading to increased performance of the system. The load transfer behaviour can further be confirmed through displacement contour in geocell reinforcement as presented in Fig. 12. It can be clearly seen that the large part of geocell reinforcement remains unaffected in case of anchor aspect ratio of 1 (Fig. 12a). Whereas, anchor having aspect ratio of 4, the entire geocell reinforcement

involved and mobilises higher resistance at soil-geocell interface thereby enhances the performance of the system. This generally agrees with the pullout load-displacement response and the displacement contours that was discussed earlier. Hence, it can be said that the geocell reinforcement is effectively resisted the anchor load even for larger aspect ratio of an anchor plate. These findings are consistent with the reported response of pullout factor vs. anchor aspect ratio as shown in Fig. 8.

Practical Implication and Limitation of the Present Study

The current analysis makes it quite evident that the anchor plate's ability to support loads is strongly impacted by the aspect ratio of plate anchor. Further, the performance of vertical plate anchors significantly increases in the range of 146%-227% with the engineering behaviour of the geocell reinforcement for different aspect ratios of an anchor plate. However, the maximum performance improvement was found to be nearly 227% for an aspect ratio (i.e., L/h) of 3, demonstrating that the rectangular anchor plate having an aspect ratio of 3 placed in geocell reinforced soil mass performed better among others. The findings of this study are highly beneficial for mitigating lateral displacement in various earth-retaining structures, including anchored retaining walls, sheet pile walls, bulkheads, and bridge abutments. Additionally, the results offer practical guidance for the design and construction of geocell-reinforced anchored systems.

A 3D numerical model, implemented in PLAXIS 3D, was utilized to assess the impact of anchor plates on geocell-reinforced soil systems. First, by comparing the suggested model to the current experimental investigation, its accuracy was assessed (Dash and Choudhary, 2018). The obtained results closely aligned with previously reported experimental findings. The numerical results for the square anchor plate closely match the experimental findings, confirming that the proposed model is suitable for analyzing the impact of various parameters on the anchor plate system's overall performance. However, for better accuracy experimental

model test need to be performed considering wide range of anchor sizes. Besides, the effect of varying anchor plate stiffness was not explored in this study, and all analyses were conducted and reported assuming a rigid anchor plate in the numerical model.

Conclusion

This study presents numerical analysis on the behaviour of geocell reinforced vertical anchor plate using three-dimensional finite element method PLAXIS 3D. Initially, the proposed numerical models for reinforced anchor system are validated with the reported model test results; subsequently detailed analyses have been performed. This study focuses on examining how the aspect ratio of vertical plate anchors in geocell-reinforced soil beds affects enhanced system performance. The findings of the study lead to the following inferences.

1. The results obtained from three-dimensional numerical analysis for both unreinforced and reinforced vertical square anchor plate system shows good coherence with the reported experimental results, indicating that the proposed model can be used to study the influence of geometry of an anchor plate placed in geocell reinforced soil system.
2. Regardless of the anchor plate's aspect ratio, geocell reinforcement markedly boosts the vertical plate anchor system's performance, increasing capacity by 146% to 227%. This enhancement stems from the geocell's semi-rigid structure, which distributes anchor loads across a broader soil area, thereby elevating the system's overall resistance. Further, it has been noticed that the maximum performance improvement found to be nearly 227% for anchor aspect ratio of (i.e., L/h) of 3 demonstrating that the rectangular anchor plate having aspect ratio of 3 placed in geocell reinforced soil mass performed better among others.

3. The uplift resistance of both unreinforced and geocell-reinforced vertical plate anchors increases as the aspect ratio (L/h) of the plate increases. However, the non-dimensional pullout factor found to be decreases significantly with an increase in aspect ratio up to L/h = 5 for both unreinforced and geocell reinforced case, beyond which, further reduction was found to be marginal. Therefore, it can be said that the square anchor behavior shifted to strip anchor behavior beyond aspect ratio (i.e., L/h) of 5 both for unreinforced and reinforced case indicating that the influence of aspect ratio of anchor plate is nearly same in both the cases.
4. The pattern of displacement contour for all the cases was found to be nearly same that is, it generated from the bottom edge of the anchor plate, extended laterally and finally reached to the ground surface. However, the flow of soil element confined within the geocell mattress for an anchor aspect ratio L/h = 1 and extended beyond the geocell reinforcement for L/h = 4 indicating that larger size of anchor plate disperse the upcoming load over larger area leading enlarge failure surface thereby mobilising enhanced resistance in the vicinity of geocell reinforced anchor beds leading to increased performance of the system.
5. The pattern of tensile stresses developed within the wall of the geocell under horizontal pullout loading clearly indicates that the tensile forces are developed on the front face of the geocell walls and very concentrated all around the anchor plate in case L/h = 1. Whereas, almost entire geocell mattress experiences tensile forces for aspect ratio of 4, indicating that with increase in the aspect ratio, the large portion of composite structures (i.e., geocell reinforced system) involve in sharing anchor load thereby enhances the overall performance of the system. Thus, geocell reinforcement effectively withstands horizontal pullout loads on anchor plates, even for those with higher aspect ratios.

The results of this research demonstrate that geocell reinforcement significantly enhances the stability and functionality of anchored system. Further, it will help to decide the optimum aspect ratio of anchor plate to be used for geocell reinforced anchored structures. The presented investigation will also help researchers to comprehend the insight mechanism of geocell reinforced anchor system to conduct their research work in this field. Nevertheless, the field study requires to be conducted to get realistic results.

Conflict of interest

On behalf of all authors, the corresponding author declares that there is no conflict of interest.

Acknowledgement

The authors would like to express sincere gratitude to all the anonymous reviewers for their valuable suggestion for improving the manuscript.

List of symbols

Notation	Description
A	Area of anchor plate
B	Width of anchor plate
H	Embedment depth of vertical anchor plate
L	Length of anchor plate
h	Height of vertical anchor plate
H/h	Embedment ratio of vertical anchor plate
d/h	Anchor displacement
L/h	Aspect ratio
t	Thickness of anchor plate
N_u	Pullout factor
Q	Pullout load
ϕ	Angle of internal friction of soil
E	Young's modulus of soil
υ	Poisons ratio
c	Cohesion of soil
ψ	Angle of dilatancy of soil
γ	Unit weight of sand
3D	Three Dimensional

References

Ari, A. and Misir, G. (2021). "Three-dimensional numerical analysis of geocell reinforced shell foundations", Geotextile and Geomembranes 49 (4): 963-975, https://doi.org/10.1016/j.geotexmem.2021.01.006

Choudhary, A.K., Pandit, B. and Babu, G.L.S. (2019). "Three-dimensional analysis of vertical square anchor plate in cohesionless soil", Geomechanics and Geo-engineering, DOI: 10.1080/17486025.2019.16012.

Dash, S.K. (2010). "Influence of relative density of soil performance of geocell-reinforced sand foundations", Journal of Materials in Civil Engineering Div. 22 (5), 533–538 ASCE, DOI: 10.1061/(ASCE)MT.1943-5533.0000040.

Das, B.M. and Shukla, S.K. (2013). Earth anchors. 2nd ed. J. Ross Publishing, Inc., Plantation, Fla.

Dash, S.K. and Choudhary, A.K. (2018). "Geocell reinforcement for performance improvement of vertical anchor plates in sand", Geotextiles and Geomembranes. 46: 214–225, DOI: 10.1016/j.geotexmem.2017.11.008.

Dash, S.K. and Choudhary, A.K. (2019). "Pullout behavior of geocell-reinforced vertical anchor plates under lateral loading", International Journal of Geomechanics. 19(8): 04019082. © ASCE, ISSN 1532-3641, DOI: 10.1061/(ASCE)GM.1943-5622.0001452.

Ghaly, A.M. (1997). “Load-displacement prediction for horizontally loaded vertical plates”, Journal of Geotechnical and Geoenvironmental Engineering, 123-747, https://doi.org/10.1061/(ASCE)1090-0241(1997)123:1(74).

Hegde, A. and Sitharam, T.G. (2015a). “3-Dimensional numerical modelling of geocell reinforced sand beds”, Geotextiles and Geomembranes, 43, 171–18, https://doi.org/10.1016/j.geotexmem.2014.11.009.

Hegde, A. and Sitharam, T.G. (2015b). “Three-dimensional numerical analysis of geocell reinforced soft clay beds by considering the actual geometry of geocell pockets”, Canadian Geotechnical Journal, 52, 1396–1407, DOI:10.1139/cgj-2014-0387.

Ilamparuthi, K., PT, Ravichandran. and M, Toufeeq Mohammed. (2008). “Study on uplift behaviour of anchor plate in geogrid reinforced sand bed”, Geotechnical Earthquake Engineering and Soil Dynamics IV, https://doi.org/10.1061/40975(318)11.

Indraratna, B., Biabani, M. and Nimbalkar, S. (2015), “Behavior of geocell-reinforced subballast subjected to cyclic loading in plane-strain condition”, Journal of Geotechnical and Geoenvironmental Engineering 141 (1) ASCE, 04014081–16, https://doi.org/10.1061/(ASCE)GT.1943-5606.0001199.

Kumar, J. and Sahoo, J.P. (2012). “Upper bound solution for pullout capacity of vertical anchors in sand using finite elements and limits analysis”, International Journal of Geomechanics, 12, 333-337, DOI: 10.1061/(ASCE)GM.1943-5622.0000160.

Krishna, A. and Latha Madhavi, G. (2023). “Evolution of Geocells as Sustainable Support to Transportation Infrastructure”, Sustainability 2023, 15, 11773, https://doi.org/10.3390/su151511773.

Kumar, V., Priyadarshee, A., Chandra, S., Jindal, A. and Rana, D. (2024). "Behavioral study of raft reinforced with geogrid and geocell through experiments and neural models", Civil Engineering Infrastructures Journal 2023, 56(2): 321-332, DOI: 10.22059/CEIJ.2023.343951.1847.

LaGatta, D.P. and Shield, D.R. (1984). "Failure of an anchored sheet pile bulkhead", In: Proc. Of the First International Conference on Case Histories in Geotechnical Engineering, pp. 393–399 St. Louis, Missouri.

Mehdipour, I., Ghazavi, M., and Moayed, R. Z. (2013). "Numerical study on stability analysis of geocell reinforced slopes by considering the bending effect", Geotextiles and Geomembranes, 37, 23-34, https://doi.org/10.1016/j.geotexmem.2013.01.001.

Oliaei, M. and Kouzegaran, S. (2017). "Efficiency of cellular geosynthetics for foundation reinforcement", Geotextiles and Geomembranes, 45, 11–22., https://doi.org/10.1016/j.geotexmem.2016.11.001.

Plaxis. (2019). "Plaxis 3D Reference Manual Technology", https:// doi.org/10.1093/cid/ciq238.

Rokonuzzaman, M. and Sakai, T. (2012a). "Model tests and 3D finite element simulations of uplift resistance of shallow rectangular anchor foundations", International Journal of Geomechanics, 12(2), 105–112, DOI: 10.1061/(ASCE)GM.1943-5622.0000119.

Rokonuzzaman, M. and Sakai, T. (2012b). "Evaluation of shape effects for rectangular anchors in dense sand: model tests and 3D finite-element analysis", International Journal of Geomechanics, 12 (2), 176–181, https://doi.org/10.1061/(ASCE)GM.1943-5622.0000116.

Rahimi, M., Moghaddas Tafreshi, S.N., Leshchinsky, B. and Dawson, A.R. (2018b). "Experimental and numerical investigation of the uplift capacity of anchor plates in geocell reinforced sand", Geotextiles and Geomembranes, 46(6), 801-816, https://doi.org/10.1016/j.geotexmem.2018.07.010.

Shahriar, A. R., Islam, M. S., and Jadid, R. (2020). "Ultimate pullout capacity of vertical anchors in frictional soils", International Journal of Geomechanics, 20(2), 04019153, https://doi.org/10.1061/(ASCE)GM.1943-5622.0001576.

Song, G., Song, X., He, S., Kong, D., and Zhang, S. (2022). "Soil reinforcement with geocells and vegetation for ecological mitigation of shallow slope failure", Sustainability, 14(19), 11911. https://doi.org/10.3390/su141911911.

Tilak, V.B. and Samadhiya, N.K. (2022). "Pullout capacity of circular multi-plate vertical anchors in sand – An experimental study", Ocean Engineering 258 (2022) 111779, https://doi.org/10.1016/j.oceaneng.2022.111779.

Xing, G., Cao, Y., Zhang, B., Li, J., and Li, D. (2023). "Analytical Study on Limiting Value of Shape Factor of Vertically Loaded Anchors in Saturated Soft Clay", Advances in Civil Engineering, 2023(1), 8853093, https://doi.org/10.1155/2023/8853093.

Zhuang, P., Yue, H., Song, X., Sun, R., Wu, J. and Guan, Y. (2021). "Ultimate pullout capacity of single vertical anchor plates in sand", Marine Georesources and Geotechnology, https://doi.org/10.1080/1064119X.2021.1950247.

Zhang, S., Wang, Y., Li, C., Li, Q. and Yang, D. (2022). "Microscopic Bearing Behavior of Horizontally Loaded Vertical Anchor plates in Sandy Soil", Hindawi Advances in Civil Engineering Volume 2022, Article ID 7371229, 14 pages, https://doi.org/10.1155/2022/7371229.

List of Table

Table 1. Properties of Soil (Dash and Choudhary 2018).

Properties	RD =75%
Young's modulus (MPa)	14.5
Poisson's ratio, (ν)	0.3
Shear modulus (MPa)	5.58
Cohesion (kPa)	0
Friction angle (ϕ°)	39
Dilation angle (ψ°)	18
Unit weight (kN/m^3)	16.87

Table 2. Properties of Anchor plate and Tie Rod (Dash and Choudhary 2018).

Properties	**Anchor plate**	**Tie Rod**
Model	Linear Elastic	Linear Elastic
Structural element	Plate	Embedded Beam
Young's modulus ((kPa)	200×10^6	200×10^6
Size (mm x mm)	100 x 100	1200 (length)
Thickness (mm)	10	12 (Diameter)
Material	Mild Steel	Mild Steel
Unit weight (kN/m^3)	78.50	78.50

Table 3. Properties of Geocell Reinforcement (Dash and Choudhary 2018).

Properties	Geocell
Model	Linear Elastic
Structural element	Geogrid
Young's modulus (MPa)	470
Size of Unit Cell	100 mm x 100 mm
Height of Geocell	200 mm
Axial Stiffness (kN/m)	376

Table 4. Summary of numerical result for unreinforced vertical anchor plate.

Size of anchor plate (mm)	Peak Pullout Load (kN)	Pullout factor (N_u)
100 × 100	1.35	27.84
100 × 200	1.64	16.84
100 × 300	1.89	12.96
100 × 400	2.10	10.78
100 × 5 00	2.33	9.60
100 × 600	2.66	9.11

Table 5. Summary of numerical results for reinforced vertical anchor plate.

Size of anchor plate (mm)	Anchor displacement, d/h (%)	Pullout Load (kN)	Pullout factor (N_u)		Performance Improvement (%)
			Unreinforced	Reinforced	
100x100	20	3.89	27.84	77.31	177.69
100x200	20	5.22	16.84	51.77	207.42
100x300	20	6.41	12.96	42.41	**227.24**
100x400	20	6.91	10.78	34.28	218.00
100x500	20	7.31	9.60	29.00	202.08
100x600	20	7.69	9.11	25.43	179.14
100x700	20	7.86	9.05	22.29	146.30

List of Figures

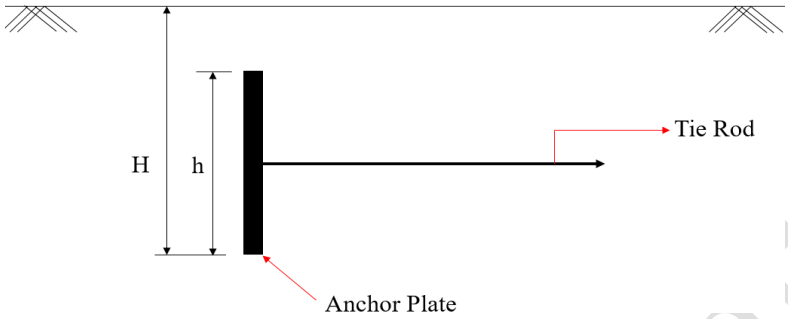

Fig. a. Cross-sectional view of an anchor plate.

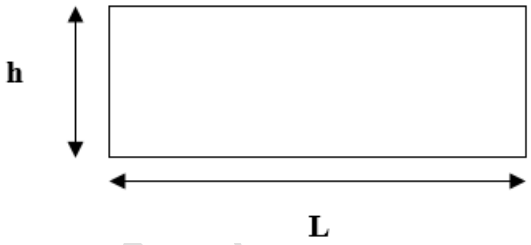

Fig. b. Plan of an anchor plate.

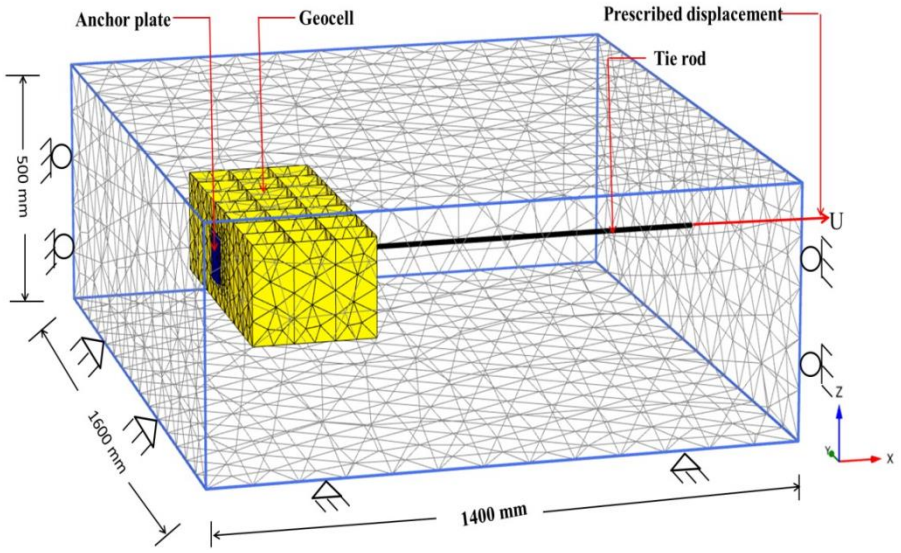

Fig. c. Schematic layout of the model with boundary condition.

Fig. 1. a. Cross-sectional view of an anchor plate. b. Plan of an anchor plate. c. Schematic layout of the model with boundary condition.

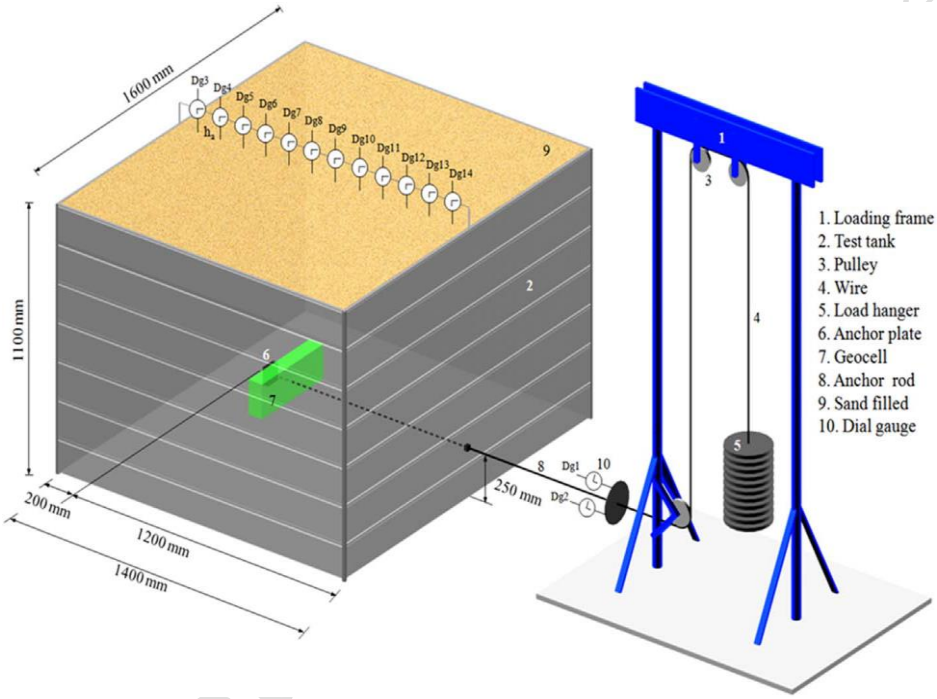

Fig. 2. Experimental setup (Dash and Choudhary 2018).

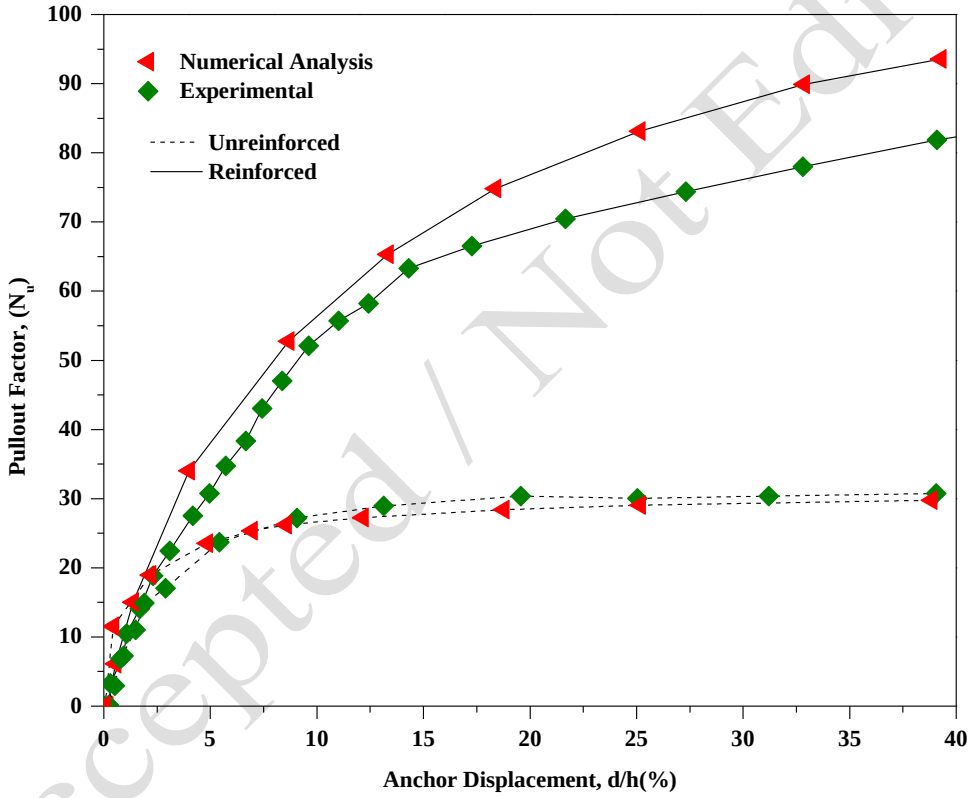

Fig. 3. Pullout factor vs. anchor displacement response.

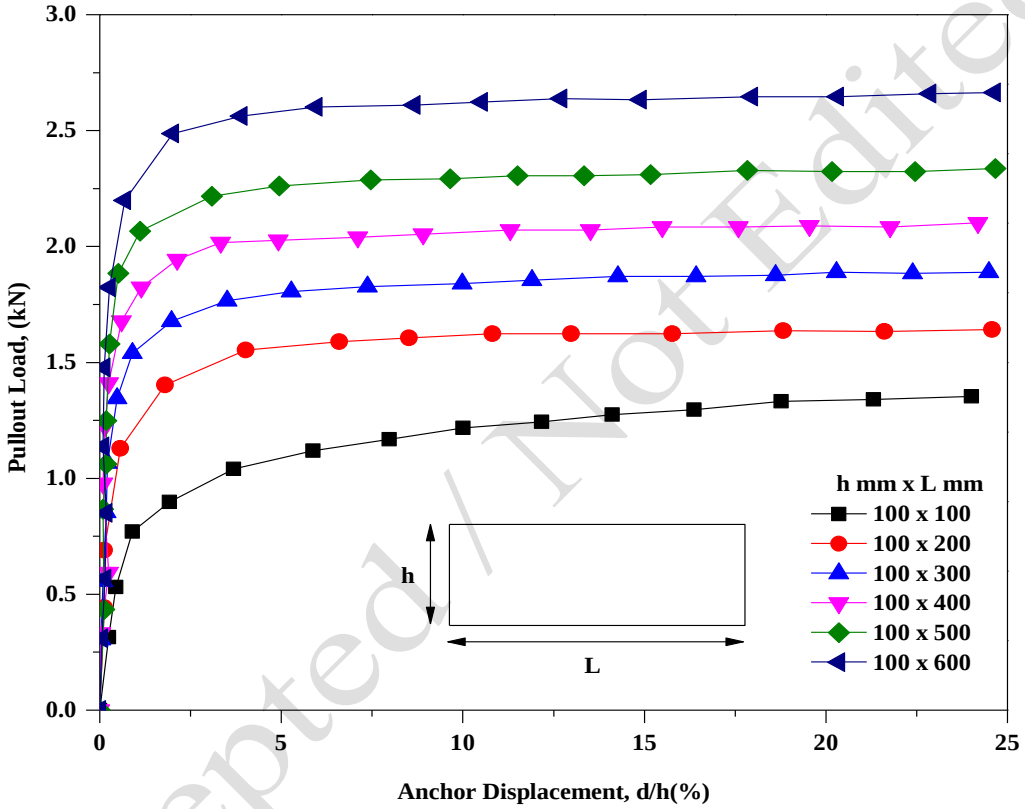

Fig. 4. Variation of pullout load vs. anchor displacement: Unreinforced case.

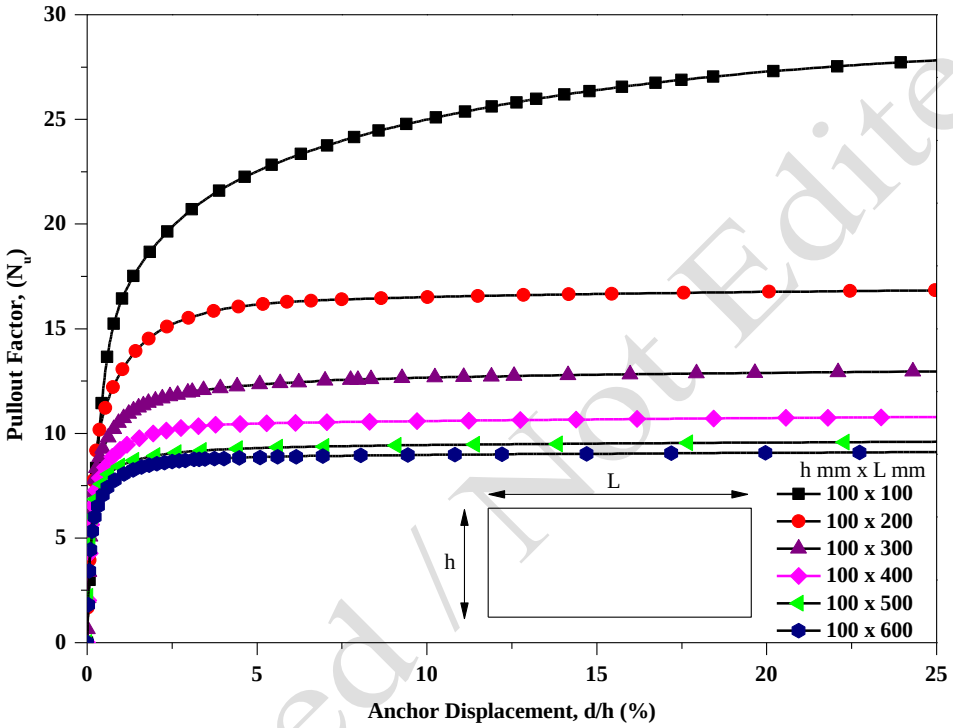

Fig. 5. Variation of pullout factor vs. anchor displacement: Unreinforced case.

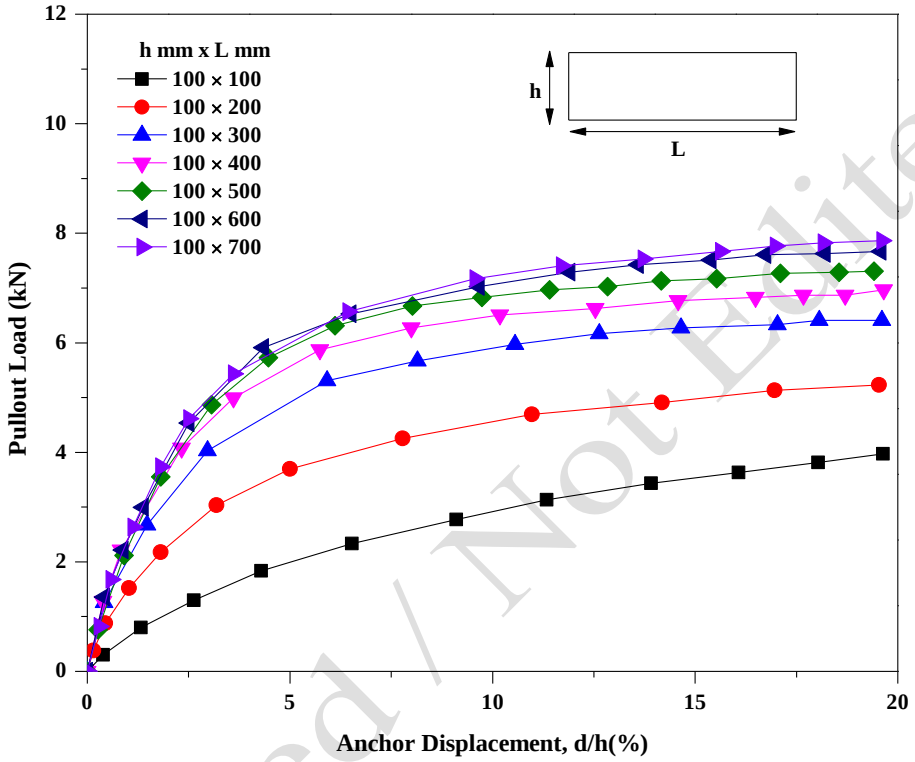

Fig. 6. Variation of pullout load vs. displacement: Reinforced Case.

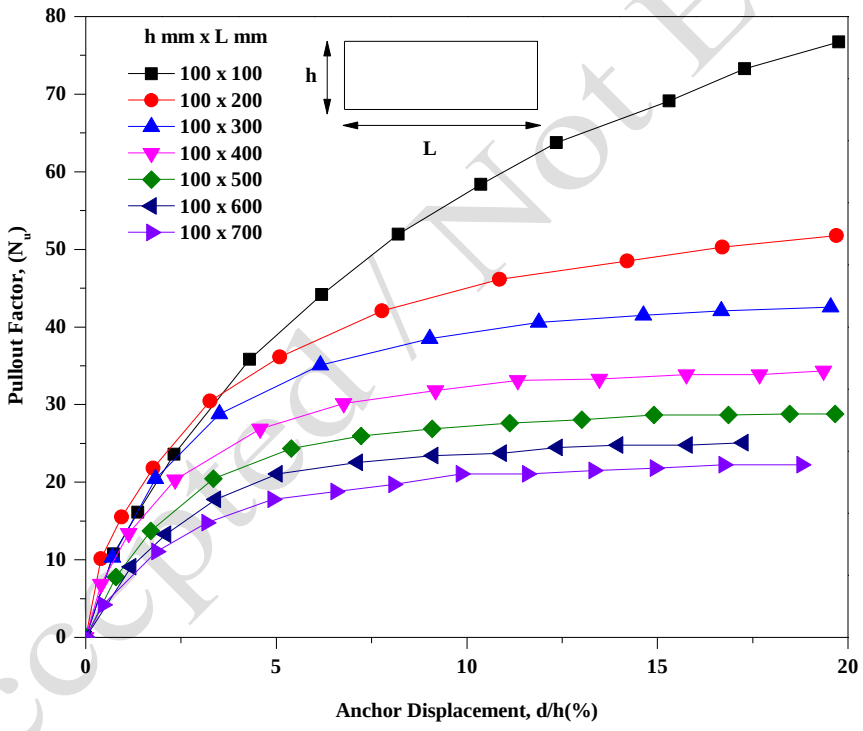

Fig. 7. Variation of pullout factor vs. anchor displacement: Reinforced Case.

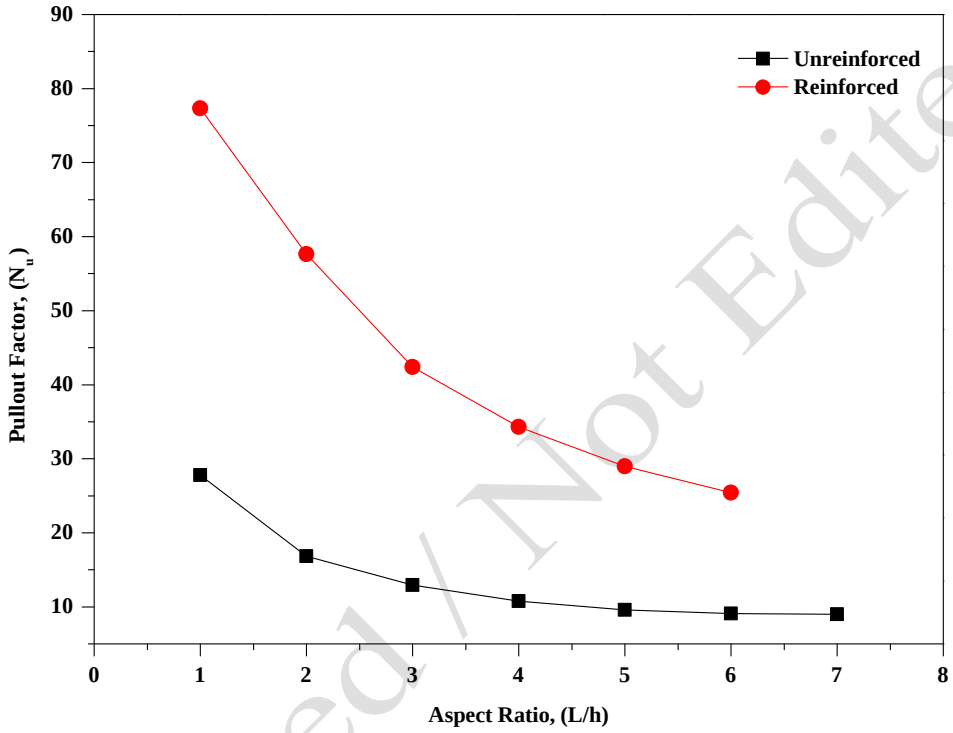

Fig. 8. Pullout factor vs. aspect ratio.

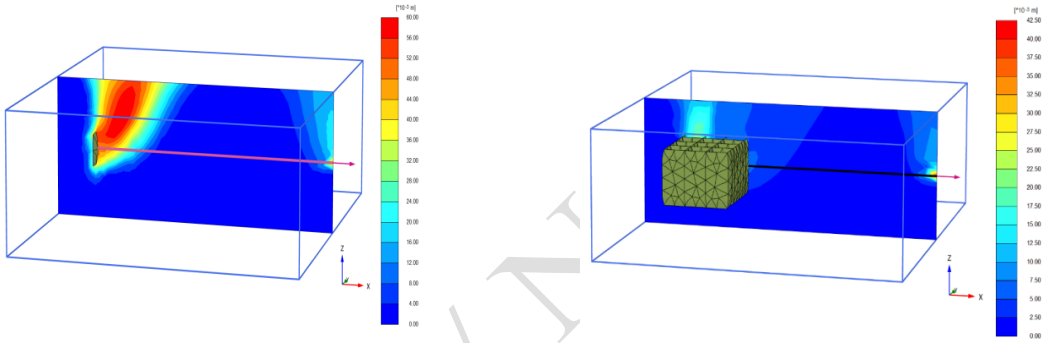

(a) Unreinforced **(b) Reinforced**

Fig. 9. Contour displacement of soil (anchor size: 100 mm x 100 mm).

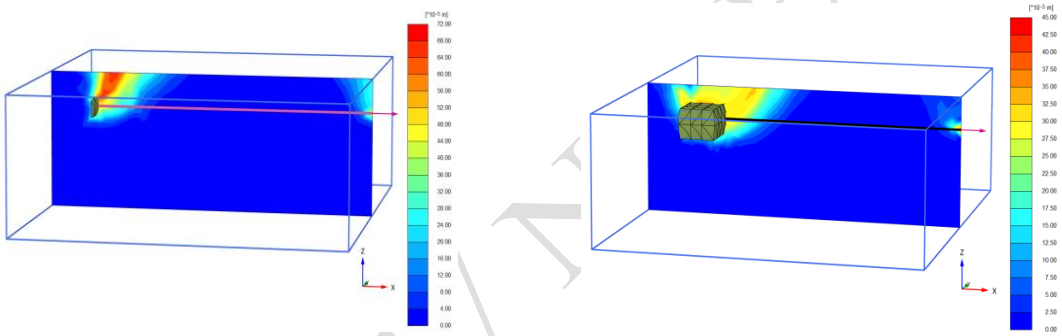

(a) Unreinforced **(b) Reinforced**

Fig. 10. Contour displacement of soil (anchor size: 100 mm x 400 mm).

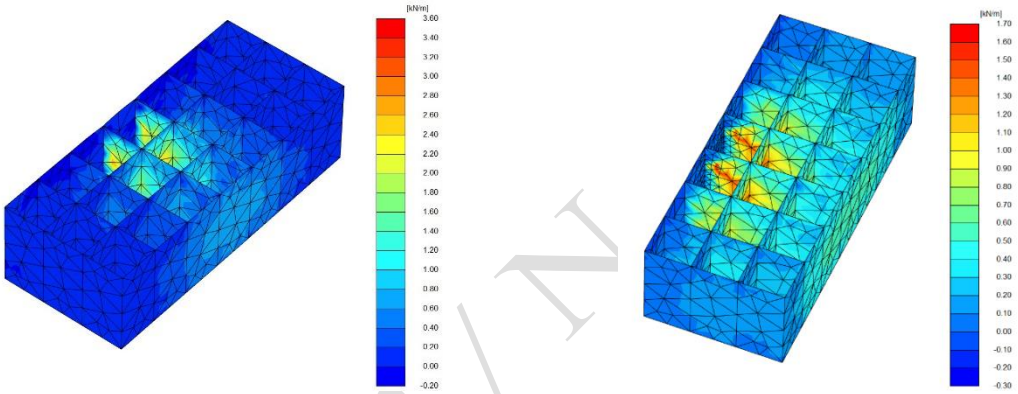

(a) Size of anchor: 100 mm x 100 mm (b) Size of anchor: 100 mm x 400 mm

Fig. 11. Distribution of tensile force on geocell.

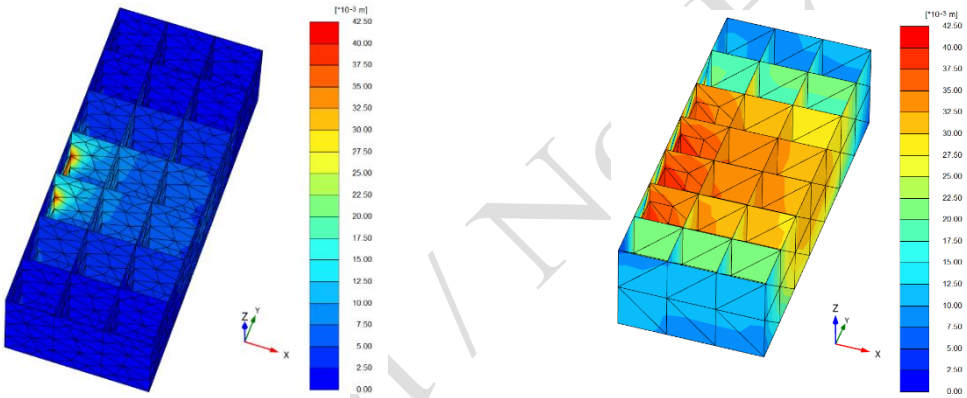

(a) Size of anchor: 100 mm x 100 mm (b) Size of anchor: 100 mm x 400 mm

Fig. 12 Distribution of displacement contour on geocell.